ACS Sustainable Chemistry & Engineering

Research Article

pubs.acs.org/journal/ascecg

Radical Nature of C-Lignin

Laura Berstis,[†] Thomas Elder,[‡] Michael Crowley,[*,†] and Gregg T. Beckham[*,†]

[†]National Bioenergy Center, National Renewable Energy Laboratory, 15013 Denver West Parkway, Golden, Colorado 80401, United States

[‡]USDA-Forest Service, Southern Research Station, 521 Devall Drive, Auburn, Alabama 36849, United States

Ⓢ *Supporting Information*

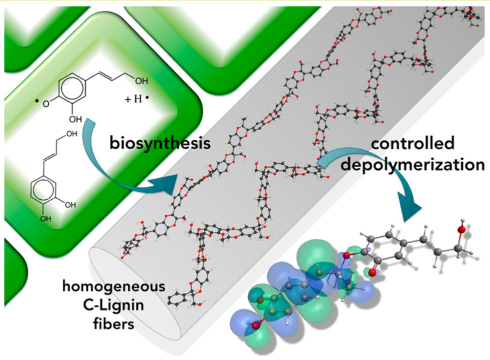

ABSTRACT: The recently discovered lignin composed of caffeoyl alcohol monolignols or C-lignin is particularly intriguing given its homogeneous, linear polymeric structure and exclusive benzodioxane linkage between monomers. By virtue of this simplified chemistry, the potential emerges for improved valorization strategies with C-lignin relative to other natural heterogeneous lignins. To better understand caffeoyl alcohol polymers, we characterize the thermodynamics of the radical recombination dimerization reactions forming the benzodioxane linkage and the bond dissociation into radical monolignol products. These properties are also predicted for the cross-coupling of caffeoyl alcohol with the natural monolignols, coniferyl alcohol, sinapyl alcohol, and *p*-coumaryl alcohol, in anticipation of polymers potentially enabled by genetic modification. The average BDEs for the C-lignin benzodioxane α- and β-bonds are 56.5 and 63.4 kcal/mol, respectively, with similar enthalpies for heterodimers. The BDE of the α-bond within the benzodioxane linkage is consistently greater than that of the β-bond in all dimers of each stereochemical arrangement, explained by the ability the α-carbon radical generated to delocalize onto the adjacent phenyl ring. Relative thermodynamics of the heterodimers demonstrates that the substituents on the phenyl ring directly neighboring the bond coupling the monolignols more strongly impact the dimer bond strengths and product stability, compared to the substituents present on the terminal phenyl ring. Enthalpy comparisons furthermore demonstrate that the *erythro* stereochemical configurations of the benzodioxane bond are slightly less thermodynamically stable than the *threo* configurations. The overall differences in strength of bonds and reaction enthalpies between stereoisomers are generally found to be insignificant, supporting that postcoupling rearomatization is under kinetic control. Projecting the lowest-energy stereoisomer internal coordinates to longer polymer C-lignin strands highlights how significantly the stereochemical outcomes in polymerization may impact the macromolecular structure and in turn material and chemical properties. Through these comparisons of geometry, bond strengths, and reaction enthalpies, we shed light on the distinctive properties of C-lignin's radical recombination and decomposition chemistry, and its potential as a natural lignin solution for biorefinery feedstocks and unique materials science applications.

KEYWORDS: *Lignin biosynthesis, Lignin valorization, Caffeoyl alcohol, Caffeyl alcohol, Bond dissociation enthalpy*

INTRODUCTION

Biofuels derived from lignocellulosic biomass hold great potential for aiding in the world's energy needs yet are confronted by several key hurdles. Biomass recalcitrance in particular impedes the economical production of cellulosic biofuels due to the inherent challenges to efficiently depolymerize both plant polysaccharides and aromatic-rich lignin polymers.[1,2] Each present unique challenges to decomposition, given that billions of years of plant evolution have optimized these polymers to present strong resistance to chemical and enzymatic degradation. Nevertheless, great strides in the cost-reduction of polysaccharides' depolymerization have been made through the optimization of a thermochemical pretreatment process[3−6] and recently dramatically improved enzyme cocktails.[7,8] In contrast, there remains significant room for improvement in developing economical processes for decomposing and sequestering high-value products from lignin.[2,9,10] As designed by nature, the heterogeneous composition and branching of this polymer create a complex chemical environment and in turn, greater difficulty in degrading in a controlled and predictable manner. However, tackling the challenge of lignin depolymerization or valorization of lignin in its polymeric form could dramatically alter the economic landscape of biofuel production.[9−12] The aromatic compounds extractable from this polymer may be upgraded to a vast array of high-value chemical or material products[2,9,10] and in turn are capable of revolutionizing the economics of cellulosic biofuels and fine chemical production from biomass.

Special Issue: Lignin Refining, Functionalization, and Utilization

Received: March 13, 2016
Revised: May 12, 2016
Published: May 17, 2016

ACS Publications

DOI: 10.1021/acssuschemeng.6b00520
ACS Sustainable Chem. Eng. 2016, 4, 5327−5335

Lignin has long been studied as an organic polymer material, with appealing capabilities for tuning its properties, for example, via the available C3 and C5 *ortho* positions on the phenyl rings available to chemical modifications. However, the heterogeneities of the molecule have complicated its widespread application.[13] In spite of its complex composition and linkages, lignin has been increasingly gaining attention as a carbon fiber precursor, due to the high carbon content of the raw material, at much lower cost than that of the current polyacrylonitrile source.[13] To date, the use of lignin as a carbon fiber precursor has generated impressively high specific surface areas, compared to that of traditional carbon activation techniques.[13−15] Lignin-based carbon fibers could be broadly applied to aerospace, sporting goods, and automotive applications if the process were made more tractable industrially and economically.[16] Similarly, in numerous other materials science areas, the interest in lignin-based materials is amassing,[13,17,18] for example, in polymer blend applications given that it has been demonstrated to improve rigidity,[9] reduce water sensitivity,[19] and stabilize against UV degradation due to the phenol groups acting as free radical scavengers.[20−22]

In most species and tissues, natural lignins are formed via the polymerization of several phenylpropanoid monomers, coniferyl alcohol (abbreviated G, for the guaiacyl lignin unit), sinapyl alcohol (S, or syringyl lignin unit), and *p*-coumaryl (H, for the hydroxyphenyl unit) (Figure 1). These monomers are polymerized through radical recombination coupling chemistry (Figure 1), which generates a diverse array of interunit linkages, including the highly prevalent *β*-O-4linkage, as well as *β*-*β*, 5-O-4, and *β*-5.[23,24] Hydroxycinnamates, including *p*-coumarate and ferulate, may also serve as monomers in grass lignins, which has importantly revealed the compatibility of natural lignification with ferulate conjugates.[25]

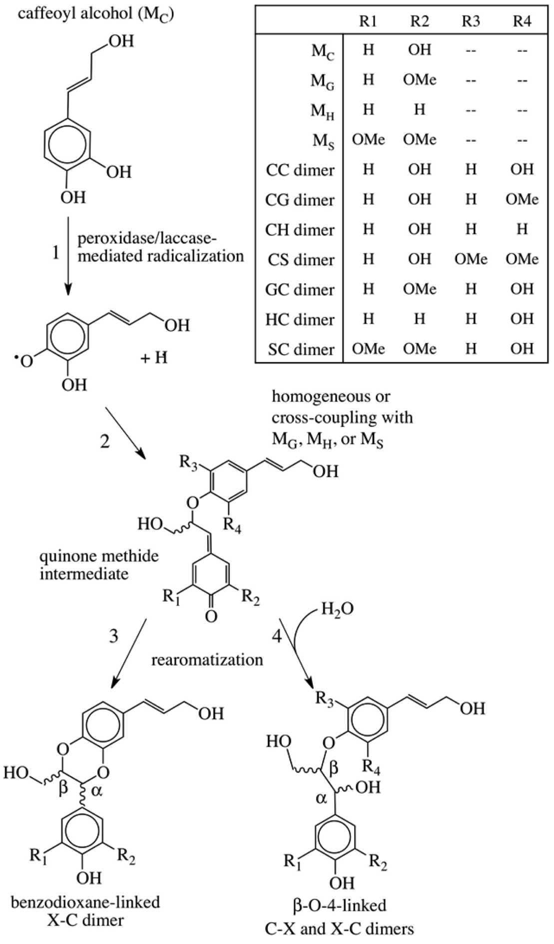

	R1	R2	R3	R4
M_C	H	OH	--	--
M_G	H	OMe	--	--
M_H	H	H	--	--
M_S	OMe	OMe	--	--
CC dimer	H	OH	H	OH
CG dimer	H	OH	H	OMe
CH dimer	H	OH	H	H
CS dimer	H	OH	OMe	OMe
GC dimer	H	OMe	H	OH
HC dimer	H	H	H	OH
SC dimer	OMe	OMe	H	OH

Figure 1. Coupling of caffeoyl alcohol homodimers or heterodimers with G-, H-, or S-lignin monolignols to *β*-O-4- or benzodioxane-linked dimers.

Engineered and novel lignins are increasingly gaining interest as a tactic to develop lignin polymers, which reduce heterogeneity and chemical complexity, while preserving the role in pathogen resistance and phenotype. Among these efforts for simplifying lignin chemistry has been the development of easily cleavable interunit bonds, such as ZIP-Lignins.[26,27] This engineering strategy introduces a feruloyl-CoA monolignol transferase gene into the tissue, which during lignin biosynthesis incorporates monolignol ferulate conjugates into the growing polymer network. These bonds are easily cleavable by mild alkaline conditions, effectively "unzipping" the polymer.[26,28] Further approaches to enhance degradability include reducing heterogeneity via knockouts of key enzymes in monolignol synthesis or other genetic modification (GM) techniques, such as shortening polymer lengths by introducing monomers lacking a *β*-carbon or 4-hydroxyl groups required for chain lengthening.[27−29] These engineering strategies hold great potential for reducing recalcitrance and simultaneously improving the value of chemical products harvested from depolymerization, through tuning the substituents of the engineered monolignol building blocks.

Additionally, an appealing alternative to GM-lignin was recently discovered: a natural lignin homopolymer of caffeoyl alcohol, C-lignin, initially discovered in the seed coat tissues of vanilla orchids and several cacti species.[30,31] C-lignin has since been found to be biosynthesized in an increasing number of natural plant tissues coexisting but independent of traditional lignin biosynthesis in over 130 species of cacti.[32] Putatively, the high concentration of C-lignin in seed coats confers the structural functions of high strength and impermeability on this tissue.[30,32] Experimental works to understand the structure and function of this polymer have identified the benzodioxane linkages as the nearly exclusive connectivity between caffeoyl monolignols. This greatly simplifies the polymer chemistry to a predictable connectivity of homogeneous monomers, therefore affording the potential for predictable, controlled decomposition, or various uses as a naturally linear biopolymer. The key properties and energetics describing these unique linkages present in C-lignin have not yet been characterized. As such, the present work addresses the need for a characterization of key C-lignin molecular properties and their impact on chemical (de)-polymerization reactions.

Prior theoretical works have contributed a wealth of information regarding the strengths of cleavable bonds in natural lignin model systems[33−38] via the predictions of relative energetics and bond dissociation enthalpies (BDEs).[34,38,39] The mechanisms by which a broad variety of linkages in lignins are formed have also been well-established through both theoretical and experimental works as the recombination of the radical monolignol species.[24,40] Whether ultimately forming the common *β*-O-4 linkage or this novel benzodioxane linkage seen in C-lignin, these radicals initially recombine to a quinone methide (QM) intermediate prior to a rearomatization, shown in reactions 3 and 4 of Figure 1.

While the *β*-O-4 linkage is formed through a hydration reaction that completes the rearomatization, the benzodioxane link formation proceeds as an entirely intramolecular process, given the availability of the 5-OH group to act as the nucleophile. The efficient intramolecular reaction mechanism helps explain why the benzodioxane linkage is the nearly exclusive connectivity found in C-lignin. It is therefore highly intriguing to study the energetics of this benzodioxane linkage with quantum mechanical theory, to elucidate the thermodynamics and BDEs of linkages with caffeoyl alcohol. We therefore have applied density functional theory (DFT) models to evaluate the relative strengths of the dimerization products of C−C homodimers and C-X lignin species (for X = guaiacyl (G), *p*-hydroxyphenyl (H), and syringyl (S) lignin subunits) in conjunction with C-lignin, as hypothetical cross-coupling products as well-characterized for the G, H, and S monolignols.[41] While cross-coupling is not observed for caffeoyl alcohol with G or S monolignols, we compare the cross-coupling to these alternative products to explore the extent to which the individual monolignol properties impact the bond strengths and thermodynamics of the dimer systems. Future GM efforts may be extended to enable this potentially advantageous nonstandard biosynthesis. Our analyses highlight the differences between C-lignin radical polymerization chemistry to its preferred benzodioxane linkage, relative to the *β*-O-4 linkage and other natural lignins. In this comparison, we address the issue of potential stereochemical effects, by individually assessing all four possible stereochemical outcomes of each dimerization.

Further of interest is an improved understanding of the macromolecular structures formed from this natural lignin polymer. Among many possible influences of structure, changes to the solvent and ion accessibility within lignin polymers would play a crucial role in the capability to either chemically or biologically degrade it into smaller high-value products. Moreover, the ability of subtle modulations in molecular level structure to impart significant material property alterations is well-known to be of great importance, despite the mystery that still enshrouds the precise interrelation of these principles.[42,43] To this effect, works of Langer and Lundquist have predicted substantial effects of lignin stereochemistry on structure.[44] We therefore extend the optimized, minimum-energy dimer structures in this study out to longer polymers holding the same internal bond angles, evaluating the extent to which the C-lignin polymer structure can differ on account of stereochemistry.

In the following sections, we present the first characterization of C-lignin bond strengths, reaction enthalpies, and structural comparisons and discuss the potential implications for the future of targeting this polymer for degradation.

■ METHODS

Initial geometries of all monomers, intermediates, and dimers were prepared and optimized in the computational chemistry software GAMESS,[45] with B3LYP/6-31+G(d,p). After confirming each to be a minimum energy structure with vibrational analyses, these provided the starting structures for conformational searches. A conformer library for each system was generated using the software TINKER,[46] which employs a hopping algorithm to search and perturb the highest vibrational modes of each conformation into new local minima along the potential energy surface for a thorough sampling of conformational space. The MMFF force fields in TINKER were applied for energetic estimates of the new conformers found in the sampling process. Structures were saved if their energies satisfied a 15 kcal/mol cutoff from the lowest-energy structure found, generating a pool of several thousand conformers for each system. As routinely performed in previous studies,[33,36,38] the 20 lowest energies of these conformers were selected for higher-level DFT optimization, using the unrestricted M06-2X/Def2-TZVPP with an ultrafine grid in Gaussian 09,[47] followed by frequency analyses to confirm that the structures had no imaginary vibrational modes. The M06-2X functional has been shown in benchmarking works to predict the thermochemical properties of similar organic systems,[48,49] as well as effective for BDE prediction in previous lignin works.[36−38] The triple-*ζ* Def2-TZVPP basis set intrinsically includes sufficient polarization and has been demonstrated to perform well for cases of unpaired electrons,[50] as is important for the enthalpy evaluations of the radical decomposition products in this study. The lowest-energy conformer of each system was selected from these refined optimizations as the approximate global minimum, and vibrational and thermal corrections at 298.15 K were calculated and included to determine the dimerization reaction enthalpies and BDEs.

The radical products resulting from hydrogen abstraction or specific bond cleavages were optimized within the same uM06-2X/Def2-TZVPP level of theory. Following the theoretical approach applied by Sangha et al.,[34,35] these structures were generated from the lowest-energy reactant (monolignol or dimer) conformation, by cleavage of the C−O or O−H bond in question, and subsequently relaxing these radical products. As such, the structural features of the reactant system are as closely preserved as possible, i.e., with no substantial alterations of noncovalent intramolecular interactions, which could misrepresent the actual strength of the bond cleaved. Thus, the most representative predictions of BDEs are found, especially relevant for modeling the case of low-temperature reactions. All vibrational analyses again confirmed that no imaginary modes existed for the unpaired-electron products, and thermal corrections were included.

The ring-opened benzodioxane systems created by the individual *α*- or *β*-bond dissociations result in an intramolecular diradical or triplet state. Low singlet−triplet gaps were found in the studies by Younker et al.,[37,38] such that treating only the triplet was found sufficient in accuracy without necessitating spin contamination corrections. These geometries were formed from decoupling either the *α*−C-O or *β*−C-O bond, opening to a torsion increased by 120°, analogous to Elder's approach of initiating a minimum 2.5 Å separation of diradicals in dibenzodioxocin ring-opened systems.[39] In this way, the nearest low-energy well in this dihedral is approximated, while separating the two radicals sufficiently to avoid recombination in the subsequent structural relaxation.

Predictions of macromolecular structures were made by propagating the internal coordinates associated with the benzodioxane-linked dimer out to 24-mer chains for each stereoisomer. As such, the optimized, lowest-energy intermonolignol linkage is modeled within a longer polymer, under the assumption that a similar intermonomer linkage would also be a preferred low-energy conformation in the polymeric form. In the linear polymer, there are no significant new interactions due to electrostatic or dispersion interactions between monomers beyond what is already present in the dimer, such that the structure is most likely to be determined by the lowest energy linkage geometries from the dimer. This zero-order approximation of the polymer geometry therefore provides a perspective of how the dimer-scale geometric preferences may manifest into larger macromolecular characteristics. These models depict the structural implications stemming from the different stereoisomers and contribute to the discussion regarding the importance of stereochemistry in lignin.

■ RESULTS AND DISCUSSION

C-Lignin Bond Strengths. Comparing initially the radical dissociation of the caffeoyl, *p*-coumaryl, coniferyl, and sinapyl monolignols, shown in Figure 2, the caffeoyl alcohol monomer dissociation enthalpy lies in a similar range as other natural monolignols. At −86.7 kcal/mol, caffeoyl alcohol compares closely to the O-4 hydroxyl BDE's of coniferyl, *p*-coumaryl, and sinapyl monomers, of 86.1, 86.4, and 82.0 kcal/mol, respectively. As shown in the singly occupied molecular orbital (SOMO) plots in Figure 2, each portrays a similar pattern of unpaired electron density onto each of the phenyl's oxygen species, ortho-, and para-positions. In turn, sinapyl alcohol has comparatively greater ability to delocalize to both the 3-OMe and 5-OMe groups.

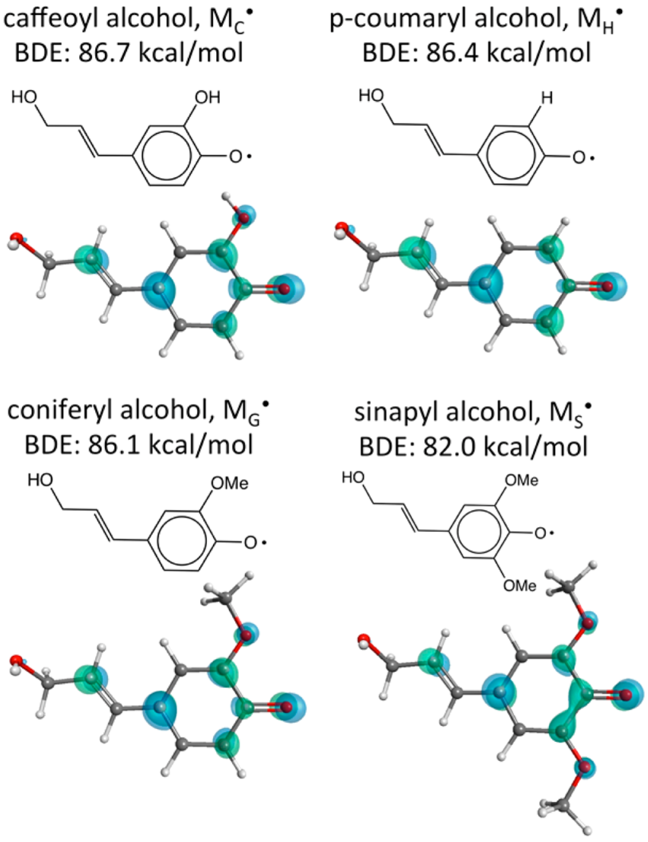

Figure 2. BDEs of monolignols to the O-4 radical precursor to polymerization, showing the SOMO of the radical products.

Presumably, this delocalization on the sinapyl alcohol enables the 4 kcal/mol stabilization with respect to the other monolignol radical abstractions.

The BDEs associated with the radical decomposition of all C-lignin homodimers and heterodimer species are presented in Table 1. For the caffeoyl alcohol homodimer, the BDEs of the benzodioxane-coupling are found to average 56.5 kcal/mol for the α-bond and 65.4 kcal/mol for the β-bond. Therefore, relative to the β-O-4 coupling mode of the C-lignin dimer, averaging at 63.6 kcal/mol, the α bond of the benzodioxane linkage is predicted to be weaker, while the β-bond is marginally stronger.

These C–O bond strengths within the benzodioxane coupling, in conjunction with the predictable, linear coupling mode, make C-lignin a highly attractive target to the growing field of lignin-based carbon fibers. The melt spinning step in carbon fiber processing requires heating to a softening temperature but mandating staying below a degradation temperature, and additives are often required for this process.[51] Hardwood lignins, tending to be more linear and have lower molecular weights than softwood, have been demonstrated advantageous in this process.[13] The further improved linearity, low molecular weight, and strong, unique coupling modality highlight C-lignin's potential to become a far superior carbon source.

Diverse biomaterial applications are similarly anticipated to benefit from these high-strength and linearity properties. Functionalization of lignin-based material, whether to alter surface chemistry properties (important for lignin-based energy storage applications),[52] or offer structural enhancements in copolymers,[53] would be greatly facilitated by the unique properties of C-lignin. For these diverse applications, the consistent monolignol chemistry and linkage type of the C-lignin polymer greatly simplifies the ability to make predictable chemical modifications to the polymer and fine-tune desired properties via substituent effects.

Breaking the α-bond yields the thermodynamically favored product due to the stabilizing delocalization of the radical electron onto the neighboring aromatic ring, as shown in the SOMO density plots in Figure 3. While the sp^2 hybridized radical α-carbon adjoins the π orbitals of the aromatic ring, the β-carbon radical (Figure 3b), is isolated from either of the phenyl ring systems by the sp^3 hybridized α-carbon. Thus, the access to the stabilizing resonance structures is inhibited, imparting a greater BDE for the β-bond.

Throughout all the caffeoyl homodimers and heterodimer systems with benzodioxane linkages, the weakness of the α-bond with respect to the β-bond is maintained, indicating that the presence of substituents on the phenyl group attached to the α-carbon do not strongly impact these BDEs. Further investigations are in progress regarding the reaction enthalpies of this benzodioxane linkage for engineered monolignols with a 5-hydroxyl group present on the phenyl to enable this coupling modality.[54] Furthermore, it remains fairly consistent that the β-bonds of the benzodioxane linkage are comparable in magnitude to the β-O-4 bond strengths, among the heterodimer species.

Comparing the BDEs of the β-O-4 heterodimers, a particular trend emerges with respect to the relative stability and the orientation of the dimer. The BDEs of the X-C heterodimers (see legend in Figure 1 for substituent positioning) correspond closely to the C–C BDEs, whereas the BDEs of the heterodimers in the C-X orientation lie on the order of ~2–5 kcal/mol higher in energy. This is indicative that the bond strength is more strongly governed by the identity of the monolignol donating its O-4 to the β-O-4 bond than the substituents present on the O-terminal phenyl ring.

Stereoisomer enthalpy differences are found to be quite small, with only a consistent trend emerging for slightly greater stabilized of the *threo* form of the benzodioxane dimer products. Between the two *erythro* (R,S) and (S,R), and two *threo* (R,R) and (S,S) forms, the BDE's vary by ~4 kcal/mol for the dissociated α-bond products and a lesser ~1 kcal/mol for the dissociated β-bond products. The impact of stereochemistry on the bond strengths is therefore taken to be considerably small. However, the very slight thermodynamic stability of the *threo* isomers may be indicative of kinetic control of the dimerization process, given the higher natural abundance of *erythro* isomers observed in some experimental studies of lignins.[55,56] Chen et al. also found a mixture of stereoisomers, i.e., no optical activity, in their inaugural characterization of C-lignin, drawing the same conclusion regarding the kinetic control of the rearomatization process.[30,31] Subtle noncovalent interactions that change in these dimers on account of the different stereocenter configurations could easily manifest these slight differences in isomer enthalpies. We further discus this observation within the context of the thermodynamic profiles of the decomposition reactions in the following section.

Relative Homo- and Heterodimer Stability. Table 2 shows the spectrum of thermodynamic stability of the different stereochemical arrangements of each dimer. The reaction enthalpies indicate that the benzodioxane coupling between caffeoyl alcohol and the C, G, H, or S monolignols is in the same range of stability as the corresponding β-O-4 products. The ΔH from the radical monomer reactants to the final product ranges 61.2–67.2 kcal/mol for the benzodioxane cases and a slightly

Table 1. Bond Dissociation Enthalpies for the Decomposition of *β*-O-4 Linked (Scheme 1) or Benzodioxane-Linked (Scheme 2) Caffeoyl Alcohol Homo- and Heterodimers with Coniferyl, Sinapyl, and *p*-Coumaryl Alcohols

Caffeoyl dimer bond dissociation reactions

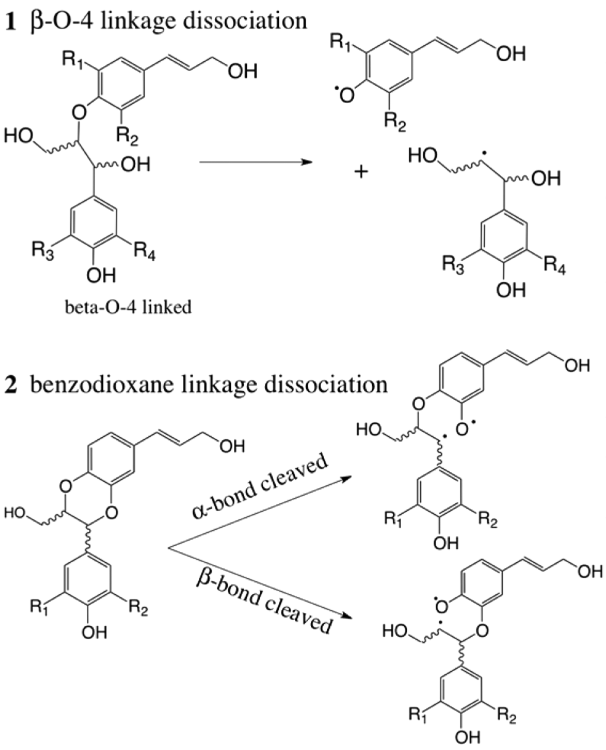

1, β-O-4 bond dissociation enthalpies, ΔH (kcal/mol)

	C-C R_1=R_3=H, R_2=R_4=OH		**C-G** R_1=H, R_2=OMe, R_3=H, R_4=OH		**C-H** R_1=R_2=H, R_3=H, R_4=OH		**C-S** R_1=R_2=OMe, R_3=H, R_4=OH
(R,R)	63.58	(R,R)	69.34	(R,R)	69.85	(R,R)	67.53
(R,S)	63.58	(R,S)	68.84	(R,S)	70.21	(R,S)	67.55
(S,R)	64.21	(S,R)	69.78	(S,R)	69.82	(S,R)	67.55
(S,S)	63.18	(S,S)	68.97	(S,S)	69.93	(S,S)	67.48

	G-C R_1=H, R_2=OH, R_3=H, R_4=OMe		**H-C** R_1=H, R_2=OH, R_3=R_4=H		**S-C** R_1=H, R_2=OH, R_3=R_4=OMe
(R,R)	63.67	(R,R)	63.84	(R,R)	63.84
(R,S)	63.67	(R,S)	63.88	(R,S)	65.39
(S,R)	63.89	(S,R)	63.89	(S,R)	65.28
(S,S)	63.89	(S,S)	63.89	(S,S)	65.05

2, Benzodioxane bond dissociation enthalpies, ΔH (kcal/mol)

		C-C R_1=H, R_2=OH		**G-C** R_1=H, R_2=OMe		**H-C** R_1=H, R_2=H		**S-C** R_1=R_2=OMe
Cα- bond cleaved	(R,R)	58.25	(R,R)	58.85	(R,R)	58.81	(R,R)	57.86
	(R,S)	55.24	(R,S)	54.22	(R,S)	54.57	(R,S)	53.37
	(S,R)	54.21	(S,R)	54.70	(S,R)	54.29	(S,R)	52.74
	(S,S)	58.44	(S,S)	58.80	(S,S)	58.86	(S,S)	58.79
Cβ bond cleaved	(R,R)	65.27	(R,R)	65.84	(R,R)	66.00	(R,R)	65.13
	(R,S)	65.50	(R,S)	64.80	(R,S)	65.24	(R,S)	65.54
	(S,R)	65.11	(S,R)	65.30	(S,R)	65.19	(S,R)	64.78
	(S,S)	65.55	(S,S)	65.80	(S,S)	66.05	(S,S)	65.54

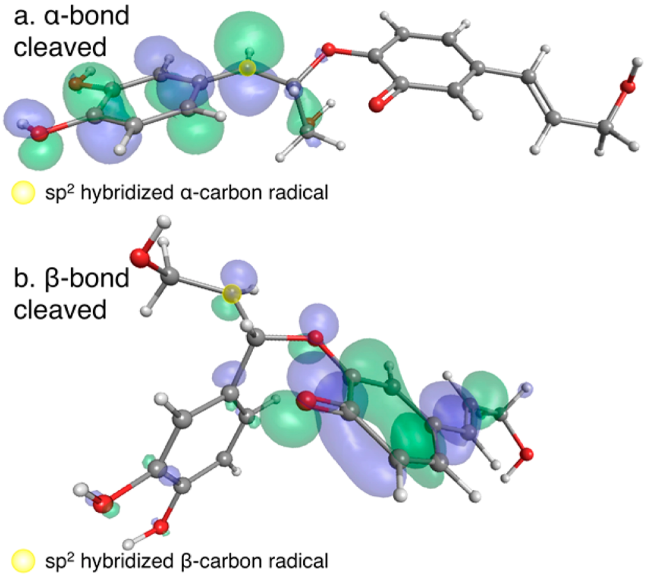

Figure 3. Highest SOMO of the benzodioxane-linked caffeoyl alcohol dimer after either cleavage of the *α*-C—O bond (top) or the *β*-C—O bond (bottom).

wider 65.7−71.4 kcal/mol range for the *β*-O-4 linkage. Similarly, the range of enthalpy stabilization moving from the QM intermediate to the benzodioxane or *β*-O-4 products is 20.5−28.7 kcal/mol and a slightly wider 19.8−33.2 kcal/mol range, respectively.

As noted with the bond dissociation to the radical monolignols, one also observes a slight difference in the thermodynamic stability of the benzodioxane-linked stereoisomers. Again, the trend shows that the R,R or S,S stereocenters on the *α*- and *β*-carbons, respectively, constitute the more thermodynamically stable products by about 2 kcal/mol relative to their *erythro* counterparts.

The series of reaction enthalpy changes along the dimerization reaction, starting from the radical monomer reactants, through the QM intermediates, and onto the benzodioxane-linked intramolecular rearomatization, or the *β*-O-4 hydration reactions, are depicted in Figure 4. Here, the average enthalpies for all stereochemical arrangements are considered. In order to place the reaction enthalpies on the same relative scale for each dimer species, the enthalpies are normalized with respect to the radical monolignol reactants.

Progressing from the radical monolignols to the QM intermediates, the C-X orientation of the heterodimers (i.e., caffeoyl alcohol lending the *β*-carbon to the newly formed bond) is generally more stabilized by the presence of substituents alongside the O-4.

Following coupling to the intermediate, the quinone methide may be rearomatized to either the benzodioxane-linked product or the *β*-O-4 product with the introduction of water. Given that no thermodynamic preference for the benzodioxane linkage was found, the C-lignin polymerization process is presumably under kinetic control creating the nearly unanimous benzodioxane-linked polymer observed experimentally.[30] The intramolecular nature of the ring closure to the benzodioxane product likely affords a highly efficient reaction. Aside from potential influences

Table 2. Enthalpies of the Different Stereoisomers of QM Intermediates, β-O-4-Linked, and Benzodioxane-Linked Dimers, Showing ΔH (kcal/mol) Values Relative to the Lowest Energy Stereoisomer

quinone methides		β-O-4 dimers, X-C	
QMcc (R)	0.00	HC (R,R)	0.05
QMcc (S)	0.04	HC (R,S)	0.06
QMcg (R)	0.00	HC (S,R)	0.00
QMcg (S)	0.00	HC (S,S)	0.00
QMgc (R)	0.00	SC (R,R)	1.18
QMgc (S)	0.00	SC (R,S)	0.00
QMch (R)	0.00	SC (S,R)	0.11
QMch (S)	0.67	SC (S,S)	0.06
QMhc (R)	0.00	GC (R,R)	0.05
QMhc (S)	0.00	GC (R,S)	0.05
QMcs R)	0.00	GC (S,R)	0.00
QMcs (S)	0.00	GC (S,S)	0.00
QMsc (R)	0.02		
QMsc (S)	0.00		
β-O-4 dimers C-X		**benzodioxane X-C dimers**	
CC (R,R)	0.00	CC (R,R)	0.00
CC (R,S)	0.00	CC (R,S)	2.31
CC (S,R)	1.20	CC (S,R)	2.41
CC (S,S)	0.42	CC (S,S)	0.26
CG (R,R)	0.10	GC (R,R)	0.00
CG (R,S)	0.00	GC (R,S)	2.03
CG (S,R)	0.00	GC (S,R)	2.15
CG (S,S)	0.47	GC (S,S)	0.03
CH (R,R)	0.09	HC (R,R)	0.04
CH (R,S)	0.53	HC (R,S)	2.07
CH (S,R)	0.12	HC (S,R)	2.05
CH (S,S)	0.00	HC (S,S)	0.00
CS (R,R)	0.02	SC (R,R)	0.06
CS (R,S)	0.00	SC (R,S)	1.96
CS (S,R)	0.00	SC (S,R)	1.90
CS (S,S)	0.06	SC (S,S)	0.00

from the reaction barriers, a faster intramolecular rearomatization step is anticipated to generate a kinetic advantage, governing the observed product preference.

Formation of the benzodioxane heterodimers is only possible with the presence of the 5-OH group on caffeoyl alcohol, such that only the X-C heterodimer orientation may be considered. Among these, the caffeoyl homodimer is the most thermodynamically stable product, closely followed by the coniferyl-caffeoyl and p-coumaryl-caffeoyl heterodimers. The sinapyl-coniferyl dimer is found to be somewhat less stable than the dimers possessing fewer substituents.

Polymer Geometric Analyses. Radical recombination of the monolignols into a growing lignin chain allows for great variety of stereochemistry to be found within lignin polymers. While Chen et al. found no optical activity in their experimental characterization of C-lignin, the different ratios of all four stereoisomers are nevertheless open to speculation.[30] Previous experimental works characterizing structural features of lignin have discussed the potentially important impact of different stereochemical products on the overall lignin properties and reactivity.[44,57−60] Langer and Lundquist have suggested that the stereochemical diversity of lignin may be among the primary factors that result in complicated NMR signals, beyond the obvious heterogeneity of linkages.[44,57,61] This corresponds to the intrinsic challenge to control the chemical decomposition reactions required for efficient and economical lignin processing.

Therefore, to investigate the sensitivity of the novel benzodioxane-linked C-lignin macrostructures to interunit stereochemistry, we generated projected linear 24-mers stemming from the lowest-energy conformations resulting from the dimer optimizations at the M06-2X/Def2-TZVPP theory level, as shown in Figure 5. The exact internal coordinates defining the intercaffeoyl-alcohol linkages were replicated between each caffeoyl unit, such that the 24-mers preserve the most stable conformations from the optimized dimers. Distinct differences in polymer curvature and length were found between the stereoisomer−pure polymers. The extent of helical-type twists of the polymer varied, with the (R,R) isomer yielding the greatest number of full rotations along the 24-mer chain. Most notably, the more compact intermonolignol configuration of the (S,S) isomer yielded a substantially compressed 24-mer polymer length of 98 Å, compared to the other configurations, each with a length of 142 Å, as measured from the terminal phenyl O4 and vinyl alcohol oxygen. This effect is further observed in the comparison of each strand's diameter, as measured by calculating the minimum radius of a cylinder to enclose the strand, where the central axis is defined by the line connecting the midpoints of the α- and β-carbons on one terminus and the O4 and O5 of the opposite terminus. This metric determines the diameter of the (S,S) stereoisomer coil to be nearly double that of the other isomers at 19.3 Å. Interestingly, these findings correlate with the predictions from combined force-field calculations and crystallographic data from Faulon et al. on the preferred conformations of β-O-4 linked stereoisomers.[62] They determine a preference of *threo* conformers to adopt a highly folded form with an intermonomer angle of 28° between the phenyl groups, opposed to the roughly 120° angles of the *erythro* isomers.[62] The present findings further support the prediction of Lundquist and Langer that the structural properties of different stereoisomers may significantly change, if sterics or environmental influences favor a more compacted arrangement.

While the difference in thermochemical stability and bond strengths in the dimers was minimal, we demonstrate here that stereochemistry can have a geometric impact on polymer structural features. These differences may, in fact, play a larger role in the efficacy of lignin degradation, given that the accessibility of catalysts and enzymes may be impacted by steric constraints in cases where the polymer exhibits a more compact geometry. Structural features such as compactness are furthermore anticipated to impact the mechanical properties of lignin-based materials, such that subtle influence of stereochemistry on polymer structure may play an important role in the fine-tuning of properties or functionalization.

Further computational and experimental analyses of lignin polymer structures may assist in better understanding the structure−reactivity relationships imparted by stereochemistry. Such information could yield valuable suggestions for improved control of polymerization as well as efficient depolymerization processes with stereospecific enzymes or catalysts. Several experimental works have demonstrated stereochemical preferences of enzymes for the synthesis and decomposition of lignin.[59] Recent works uncovered a strong stereochemical preference of β-etherases,[63,64] which could be employed for the selection of desirable stereochemistry of lignin products. Beyond its enticing structural implications, stereochemistry is therefore an attractive theme to further investigate for enhanced depolymerization potential.

DOI: 10.1021/acssuschemeng.6b00520
ACS Sustainable Chem. Eng. 2016, 4, 5327−5335

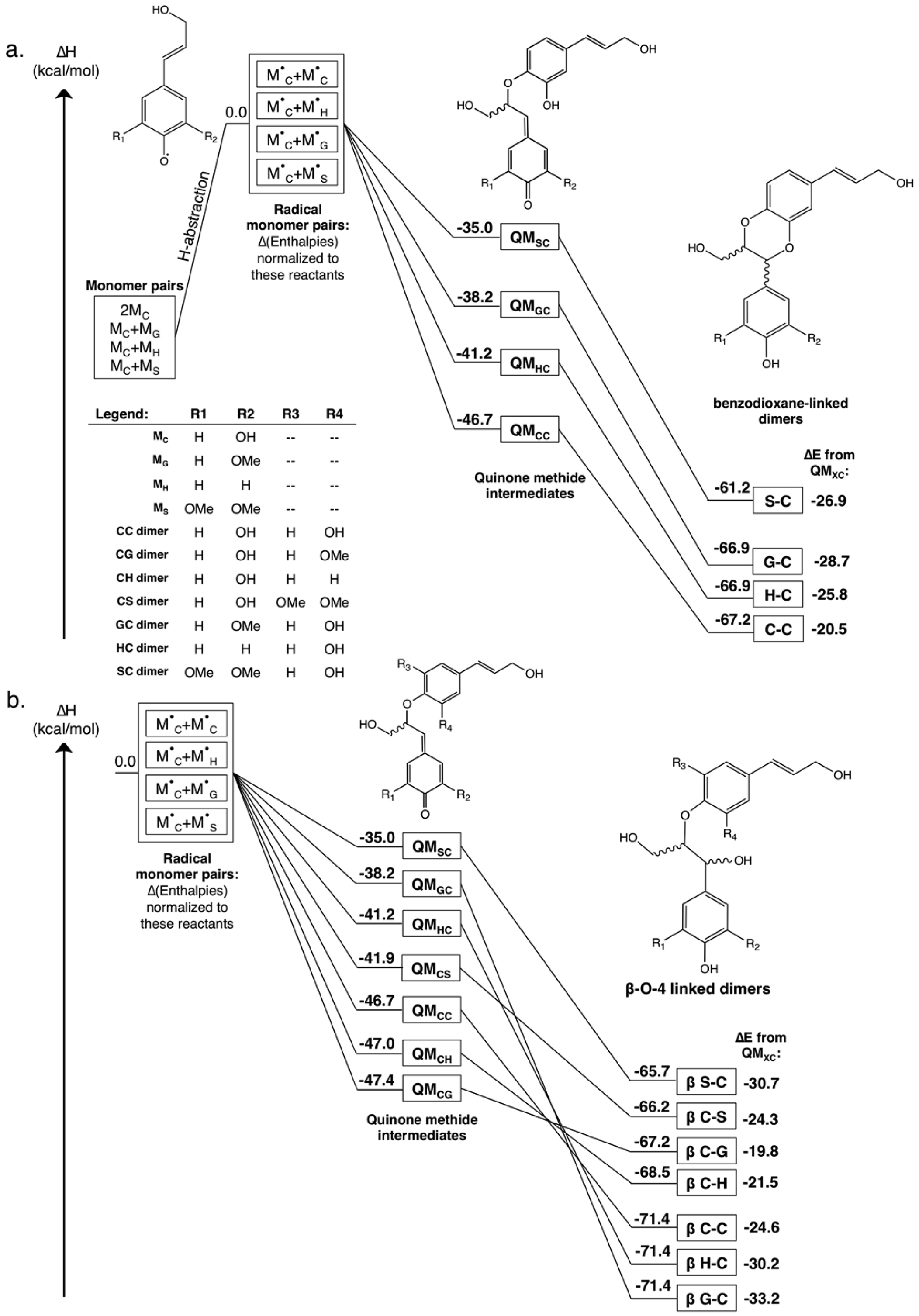

Legend:	R1	R2	R3	R4
M_C	H	OH	--	--
M_G	H	OMe	--	--
M_H	H	H	--	--
M_S	OMe	OMe	--	--
CC dimer	H	OH	H	OH
CG dimer	H	OH	H	OMe
CH dimer	H	OH	H	H
CS dimer	H	OH	OMe	OMe
GC dimer	H	OMe	H	OH
HC dimer	H	H	H	OH
SC dimer	OMe	OMe	H	OH

Figure 4. Relative thermodynamics of polymerization to (a) benzodioxane-linked and (b) *β*-O-4-linked hetero- and homodimers of caffeoyl alcohol. Enthalpy changes are normalized to the monomer radical pair reactants.

■ CONCLUSIONS

In this work, we present the first characterization of the bond strengths of the benzodioxane linkage found in C-lignin, determining that the *α*-bond is marginally weaker than the *β*-bond, similar in strength to that of the traditional *β*-O-4 linkage. Analyses of the reaction enthalpies reveal similar thermodynamic stabilities of the different homodimers and heterodimers of caffeoyl alcohol. Little to no differences in bond strengths and thermodynamic stabilities are observed between the different stereoisomers of each dimer. However, structural analyses reveal great potential for the lowest-energy conformations of each stereoisomer to adopt radically different morphologies and in turn may influence polymer properties.

Despite the higher energetic cost to fully cleave the C-lignin benzodioxane linkage, which may be a hindrance to applications necessitating decomposition, C-lignin nevertheless holds a

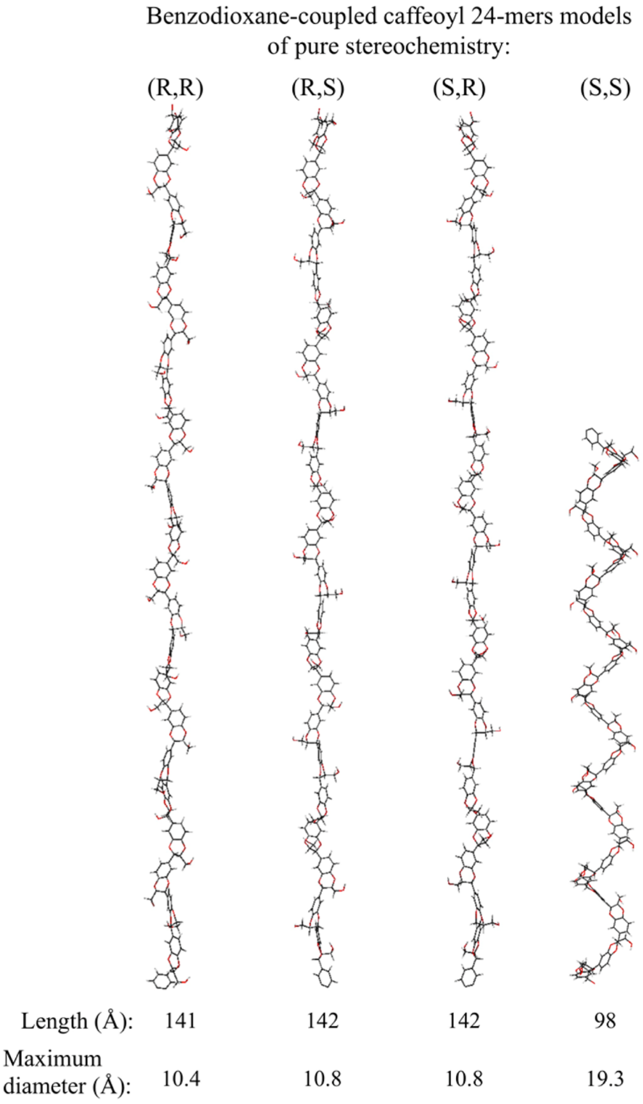

Figure 5. Projected benzodioxane-linked C−C macromolecular structures from optimized configurations of each dimer stereoisomers, with length and maximum strand diameter.

wealth of intrigue on account of its homogeneity and linearity. The benzodioxane coupling strength in fact could offer a great advantage in addition to its intrinsic linearity for diverse lignin-based biomaterials. Stereochemical effects on structure and fine-tuning with chemical modifications may both play a great role in enabling this polymer to suit the needs of many materials applications. Given its unique properties, C-lignin has the potential to become a key contender in the next generation of bioenergy solutions and in the development of high-value biomaterials.

■ ASSOCIATED CONTENT

Ⓢ Supporting Information

The Supporting Information is available free of charge on the ACS Publications website at DOI: 10.1021/acssuschemeng.6b00520.

Coordinates of optimized monomer, dimer, and 24-mer polymer geometries (PDF)

■ AUTHOR INFORMATION

Corresponding Authors

*(M.C.) E-mail: Michael.Crowley@nrel.gov.
*(G.T.B.) E-mail Gregg.Beckham@nrel.gov.

Funding

This work was supported by the US Department of Energy Bioenergy Technologies Office. We are grateful for supercomputer time on Stampede provided by the Texas Advanced Computing Center (TACC) at the University of Texas at Austin through MCB-09159 and the NREL Computational Sciences Center, which is supported by the DOE Office of EERE under Contract No. DE-AC36-08GO28308.

Notes

The authors declare no competing financial interest.

■ ABBREVIATIONS

BDE, bond dissociation enthalpy; DFT, density functional theory; C, caffeoyl alcohol; CC, caffeoyl-caffeoyl alcohol homodimer; C-X, heterodimer of caffeoyl alcohol and natural monolignol utilizing the β-carbon of the caffeoyl alcohol; X-C, heterodimer of caffeoyl alcohol and natural monolignol utilizing the O-4 of the caffeoyl alcohol; G, coniferyl alcohol (guaiacyl monolignol unit); S, sinapyl alcohol (syringyl monolignol unit); H, *p*-coumaryl alcohol (hydroxyphenyl monolignol unit); GM, genetic modification; SOMO, singly occupied molecular orbital

■ REFERENCES

(1) Himmel, M. E.; Ding, S. Y.; Johnson, D. K.; Adney, W. S.; Nimlos, M. R.; Brady, J. W.; Foust, T. D. *Science* **2007**, *315*, 804.

(2) Ragauskas, A. J.; Beckham, G. T.; Biddy, M. J.; Chandra, R.; Chen, F.; Davis, M. F.; Davison, B. H.; Dixon, R. A.; Gilna, P.; Keller, M.; Langan, P.; Naskar, A. K.; Saddler, J. N.; Tschaplinski, T. J.; Tuskan, G. A.; Wyman, C. E. *Science* **2014**, *344*, 1246843.

(3) Kumar, P.; Barrett, D. M.; Delwiche, M. J.; Stroeve, P. *Ind. Eng. Chem. Res.* **2009**, *48*, 3713.

(4) Langan, P.; Petridis, L.; O'Neill, H. M.; Pingali, S. V.; Foston, M.; Nishiyama, Y.; Schulz, R.; Lindner, B.; Hanson, B. L.; Harton, S.; Heller, W. T.; Urban, V.; Evans, B. R.; Gnanakaran, S.; Ragauskas, A. J.; Smith, J. C.; Davison, B. H. *Green Chem.* **2014**, *16*, 63.

(5) Jönsson, L. J.; Alriksson, B.; Nilvebrant, N.-O. *Biotechnol. Biofuels* **2013**, *6*, 16.

(6) Wyman, C. E. *Trends Biotechnol.* **2007**, *25*, 153.

(7) Horn, S.; Vaaje-Kolstad, G.; Westereng, B.; Eijsink, V. G. H. *Biotechnol. Biofuels* **2012**, *5*, 45.

(8) Payne, C. M.; Knott, B. C.; Mayes, H. B.; Hansson, H.; Himmel, M. E.; Sandgren, M.; Ståhlberg, J.; Beckham, G. T. *Chem. Rev.* **2015**, *115*, 1308.

(9) Kai, D.; Tan, M. J.; Chee, P. L.; Chua, Y. K.; Yap, Y. L.; Loh, X. J. *Green Chem.* **2016**, *18*, 1175.

(10) Linger, J. G.; Vardon, D. R.; Guarnieri, M. T.; Karp, E. M.; Hunsinger, G. B.; Franden, M. A.; Johnson, C. W.; Chupka, G.; Strathmann, T. J.; Pienkos, P. T.; Beckham, G. T. *Proc. Natl. Acad. Sci. U. S. A.* **2014**, *111*, 12013.

(11) Bugg, T. D. H.; Rahmanpour, R. *Curr. Opin. Chem. Biol.* **2015**, *29*, 10.

(12) Wang, P.; Dudareva, N.; Morgan, J. A.; Chapple, C. *Curr. Opin. Chem. Biol.* **2015**, *29*, 32.

(13) Duval, A.; Lawoko, M. *React. Funct. Polym.* **2014**, *85*, 78.

(14) Suhas; Carrott, P. J. M.; Ribeiro Carrott, M. M. L. *Bioresour. Technol.* **2007**, *98*, 2301.

(15) Fierro, V.; Torné-Fernández, V.; Celzard, A. *Microporous Mesoporous Mater.* **2007**, *101*, 419.

(16) Mainka, H.; Täger, O.; Körner, E.; Hilfert, L.; Busse, S.; Edelmann, F. T.; Herrmann, A. S. *J. Mater. Res. Technol.* **2015**, *4*, 283.

(17) Thakur, V. K.; Thakur, M. K.; Raghavan, P.; Kessler, M. R. *ACS Sustainable Chem. Eng.* **2014**, *2*, 1072.

(18) Upton, B. M.; Kasko, A. M. *Chem. Rev.* **2016**, *116*, 2275.

(19) Kunanopparat, T.; Menut, P.; Morel, M.-H.; Guilbert, S. *J. Appl. Polym. Sci.* **2012**, *125*, 1391.

(20) Gregorova, A.; Košíková, B.; Staško, A. *J. Appl. Polym. Sci.* **2007**, *106*, 1626.

(21) Alexy, P.; Košíková, B.; Podstránska, G. *Polymer* **2000**, *41*, 4901.

(22) Pucciariello, R.; Villani, V.; Bonini, C.; D'Auria, M.; Vetere, T. *Polymer* **2004**, *45*, 4159.

(23) Barros, J.; Serk, H.; Granlund, I.; Pesquet, E. *Ann. Bot.* **2015**, *115*, 1053.

(24) Boerjan, W.; Ralph, J.; Baucher, M. *Annu. Rev. Plant Biol.* **2003**, *54*, 519.

(25) Ralph, J. *Phytochem. Rev.* **2010**, *9*, 65.

(26) Wilkerson, C. G.; Mansfield, S. D.; Lu, F.; Withers, S.; Park, J. Y.; Karlen, S. D.; Gonzales-Vigil, E.; Padmakshan, D.; Unda, F.; Rencoret, J.; Ralph, J. *Science* **2014**, *344*, 90.

(27) Eudes, A.; Liang, Y.; Mitra, P.; Loque, D. *Curr. Opin. Biotechnol.* **2014**, *26*, 189.

(28) Mottiar, Y.; Vanholme, R.; Boerjan, W.; Ralph, J.; Mansfield, S. D. *Curr. Opin. Biotechnol.* **2016**, *37*, 190.

(29) Eudes, A.; George, A.; Mukerjee, P.; Kim, J. S.; Pollet, B.; Benke, P. I.; Yang, F.; Mitra, P.; Sun, L.; Cetinkol, O. P.; Chabout, S.; Mouille, G.; Soubigou-Taconnat, L.; Balzergue, S.; Singh, S.; Holmes, B. M.; Mukhopadhyay, A.; Keasling, J. D.; Simmons, B. A.; Lapierre, C.; Ralph, J.; Loque, D. *Plant Biotechnol. J.* **2012**, *10*, 609.

(30) Chen, F.; Tobimatsu, Y.; Havkin-Frenkel, D.; Dixon, R. A.; Ralph, J. *Proc. Natl. Acad. Sci. U. S. A.* **2012**, *109*, 1772.

(31) Chen, F.; Tobimatsu, Y.; Jackson, L.; Nakashima, J.; Ralph, J.; Dixon, R. A. *Plant J.* **2013**, *73*, 201.

(32) Tobimatsu, Y.; Chen, F.; Nakashima, J.; Escamilla-Trevino, L. L.; Jackson, L.; Dixon, R. A.; Ralph, J. *Plant Cell* **2013**, *25*, 2587.

(33) Kim, S.; Chmely, S. C.; Nimos, M. R.; Bomble, Y. J.; Foust, T. D.; Paton, R. S.; Beckham, G. T. *J. Phys. Chem. Lett.* **2011**, *2*, 2846.

(34) Sangha, A. K.; Davison, B. H.; Standaert, R. F.; Davis, M. F.; Smith, J. C.; Parks, J. M. *J. Phys. Chem. B* **2014**, *118*, 164.

(35) Sangha, A. K.; Parks, J. M.; Standaert, R. F.; Ziebell, A.; Davis, M.; Smith, J. C. *J. Phys. Chem. B* **2012**, *116*, 4760.

(36) Elder, T. *Energy Fuels* **2013**, *27*, 4785.

(37) Younker, J. M.; Beste, A.; Buchanan, A. C. *ChemPhysChem* **2011**, *12*, 3556.

(38) Younker, J. M.; Beste, A.; Buchanan, A. C. *Chem. Phys. Lett.* **2012**, *545*, 100.

(39) Elder, T. *Energy Fuels* **2014**, *28*, 1175.

(40) Vanholme, R.; Demedts, B.; Morreel, K.; Ralph, J.; Boerjan, W. *Plant Physiol.* **2010**, *153*, 895.

(41) Lu, F.; Marita, J. M.; Lapierre, C.; Jouanin, L.; Morreel, K.; Boerjan, W.; Ralph, J. *Plant Physiol.* **2010**, *153*, 569.

(42) Le, T.; Epa, V. C.; Burden, F. R.; Winkler, D. A. *Chem. Rev.* **2012**, *112*, 2889.

(43) Jancar, J.; Douglas, J. F.; Starr, F. W.; Kumar, S. K.; Cassagnau, P.; Lesser, A. J.; Sternstein, S. S.; Buehler, M. J. *Polymer* **2010**, *51*, 3321.

(44) Langer, V.; Lundquist, K.; Parkas, J. *Bioresources* **2007**, *2*, 590.

(45) Schmidt, M. W.; Baldridge, K. K.; Boatz, J. A.; Elbert, S. T.; Gordon, M. S.; Jensen, J. H.; Koseki, S.; Matsunaga, N.; Nguyen, K. A.; Su, S.; Windus, T. L.; Dupuis, M.; Montgomery, J. A. *J. Comput. Chem.* **1993**, *14*, 1347.

(46) Ponder, J. W.; Richards, F. M. *J. Comput. Chem.* **1987**, *8*, 1016.

(47) Frisch, M. J.; Trucks, G. W.; Schlegel, H. B.; Scuseria, G. E.; Robb, M. A.; Cheeseman, J. R.; Scalmani, G.; Barone, V.; Mennucci, B.; Petersson, G. A.; Nakatsuji, H.; Caricato, M.; Li, X.; Hratchian, H. P.; Izmaylov, A. F.; Bloino, J.; Zheng, G.; Sonnenberg, J. L.; Hada, M.; Ehara, M.; Toyota, K.; Fukuda, R.; Hasegawa, J.; Ishida, M.; Nakajima, T.; Honda, Y.; Kitao, O.; Nakai, H.; Vreven, T.; Montgomery, J. A., Jr.; Peralta, J. E.; Ogliaro, F.; Bearpark, M. J.; Heyd, J.; Brothers, E. N.; Kudin, K. N.; Staroverov, V. N.; Kobayashi, R.; Normand, J.; Raghavachari, K.; Rendell, A. P.; Burant, J. C.; Iyengar, S. S.; Tomasi, J.; Cossi, M.; Rega, N.; Millam, N. J.; Klene, M.; Knox, J. E.; Cross, J. B.; Bakken, V.; Adamo, C.; Jaramillo, J.; Gomperts, R.; Stratmann, R. E.; Yazyev, O.; Austin, A. J.; Cammi, R.; Pomelli, C.; Ochterski, J. W.; Martin, R. L.; Morokuma, K.; Zakrzewski, V. G.; Voth, G. A.; Salvador, P.; Dannenberg, J. J.; Dapprich, S.; Daniels, A. D.; Farkas, Ö.; Foresman, J. B.; Ortiz, J. V.; Cioslowski, J.; Fox, D. J. *Gaussian 09*; Gaussian, Inc.: Wallingford, CT, 2009.

(48) Hohenstein, E. G.; Chill, S. T.; Sherrill, C. D. *J. Chem. Theory Comput.* **2008**, *4*, 1996.

(49) Zhao, Y.; Truhlar, D. G. *Theor. Chem. Acc.* **2008**, *120*, 215.

(50) Weigend, F.; Ahlrichs, R. *Phys. Chem. Chem. Phys.* **2005**, *7*, 3297.

(51) Chatterjee, S.; Jones, E. B.; Clingenpeel, A. C.; McKenna, A. M.; Rios, O.; McNutt, N. W.; Keffer, D. J.; Johs, A. *ACS Sustainable Chem. Eng.* **2014**, *2*, 2002.

(52) Liu, W.-J.; Jiang, H.; Yu, H.-Q. *Green Chem.* **2015**, *17*, 4888.

(53) Ten, E.; Vermerris, W. *J. Appl. Polym. Sci.* **2015**, *132*, n/a.

(54) Elder, T.; Berstis, L.; Crowley, M.; Beckham, G. T., *Manuscript in preparation*.

(55) Akiyama, T.; Goto, H.; Nawawi, D. S.; Syafii, W.; Matsumoto, Y.; Meshitsuka, G. *Holzforschung* **2005**, *59*.

(56) Jönsson, L.; Karlsson, O.; Lundquist, K.; Nyman, P. O. *FEBS Lett.* **1990**, *276*, 45.

(57) Lundquist, K.; Stomberg, R. *Acta Chem. Scand.* **1987**, *41*, 610.

(58) Stomberg, R.; Lundquist, K. *J. Crystallogr. Spectrosc. Res.* **1989**, *19*, 331.

(59) Jonsson, L.; Karlsson, O.; Lundquist, K.; Nyman, P. O. *FEBS Lett.* **1990**, *276*, 45.

(60) Hishiyama, S.; Otsuka, Y.; Nakamura, M.; Ohara, S.; Kajita, S.; Masai, E.; Katayama, Y. *Tetrahedron Lett.* **2012**, *53*, 842.

(61) Lundquist, K.; Li, L. V.; Stomberg, R. *Proceedings of the Twelfth International Symposium on Wood and Pulping Chemistry*; U. Wisconsin-Madison Press: Madison, WI, 2003; Vol. *1*, pp 239.

(62) Faulon, J.-L.; Hatcher, P. G. *Energy Fuels* **1994**, *8*, 402.

(63) Picart, P.; de María, P. D.; Schallmey, A. *Front. Microbiol.* **2015**, *6*.

(64) Gall, D. L.; Ralph, J.; Donohue, T. J.; Noguera, D. R. *Environ. Sci. Technol.* **2014**, *48*, 12454.